Published in final edited form as:
Neuroimage. 2008 September 1; 42(3): 1214–1225. doi:10.1016/j.neuroimage.2008.05.028.

Group independent component analysis of language fMRI from word generation tasks

Yanmei Tie, PhD[1,2], **Stephen Whalen, BS**[2], **Ralph O Suarez, PhD**[1,2,3], and **Alexandra J Golby, MD**[1,2,3]

1*Harvard Medical School*

2*Department of Neurosurgery, Brigham and Women's Hospital*

3*Department of Radiology, Brigham and Women's Hospital*

Abstract

Language fMRI has been used to study brain regions involved in language processing and has been applied to pre-surgical language mapping. However, in order to provide clinicians with optimal information, the sensitivity and specificity of language fMRI needs to be improved. Type II error of failing to reach statistical significance when the language activations are genuinely present may be particularly relevant to pre-surgical planning, by falsely indicating low surgical risk in areas where no activations are shown. Furthermore, since the execution of language paradigms involves cognitive processes other than language function *per se*, the conventional general linear model (GLM) method may identify non-language-specific activations. In this study, we assessed an exploratory approach, independent component analysis (ICA), as a potential complementary method to the inferential GLM method in language mapping applications. We specifically investigated whether this approach might reduce type II error as well as generate more language-specific maps. Fourteen right-handed healthy subjects were studied with fMRI during two word generation tasks. A similarity analysis across tasks was proposed to select components of interest. Union analysis was performed on the language-specific components to increase sensitivity, and conjunction analysis was performed to identify language areas more likely to be essential. Compared with GLM, ICA identified more activated voxels in the putative language areas, and signals from other sources were isolated into different components. Encouraging results from one brain tumor patient are also presented. ICA may be used as a complementary tool to GLM in improving pre-surgical language mapping.

Keywords

fMRI; independent component analysis (ICA); language; pre-surgical planning

INTRODUCTION

Functional magnetic resonance imaging (fMRI) has the potential to fully observe the working of the human language system (Binder, 1997a; 2000). Information from language task fMRI can be used to non-invasively lateralize (Binder et al., 1996; Woermann et al., 2003) and

Address for correspondence: Alexandra J Golby, MD, Department of Neurosurgery, Brigham and Women's Hospital, 75 Francis Street, Boston, MA 02115, E-mail: agolby@bwh.harvard.edu, Telephone: 617-525-6776, Fax: 617-713-3050.

localize (Carpentier et al., 2001; Brannen et al., 2001) language regions in the brain. Language fMRI is also applied to define spatial relationships between brain lesions and language areas for pre-surgical mapping (Stippich et al., 2007). The sensitivity and specificity of language fMRI are major concerns in generating language maps for clinical use (Tharin and Golby, 2007). In fMRI data analysis, the conventional confirmatory analysis technique (i.e., general linear model, GLM) generates statistical maps by contrasting two conditions or comparing event-related changes to a control state (Friston et al., 1995). The null hypothesis is "no activation", and type I error of finding activations by chance is controlled by criteria of statistical significance selected by the investigator. However in pre-surgical mapping applications, an excessively conservative criterion used to identify activations in the functional areas has the potential of falsely indicating absence of surgical risk by removing the activated voxels genuinely associated with the task (Loring et al., 2002). This kind of type II error of failing to obtain statistical significance when the effects are genuinely present is particularly relevant to pre-surgical functional mapping, in order to avoid harming critical cortical areas during surgery.

A variety of word generation tasks have been used for mapping of language-specific cortical regions (Bookheimer, 2007). In such tasks, subjects are given a word or letter cue and instructed to produce a word or several words associated with the stimulus (Binder, 1997b). Since the execution of such language paradigms necessarily involves cognitive processes and sensory/motor functions other than language function *per se*, the statistical maps may show activations in the non-language-specific regions related to perceptual, attentional, motor, or other processes.

In an effort to improve pre-surgical language mapping by addressing the above problems, we investigated an exploratory method, independent component analysis (ICA), as a complementary approach to the confirmatory method (GLM). We evaluated ICA's overall ability in localizing putative language regions, both for reducing type II error and distinctly identifying language-specific regions.

ICA has been shown to be useful in the extraction of statistically independent features from fMRI data (McKeown et al., 1998; Calhoun et al., 2001a; Duann et al., 2002; Seifritz et al., 2002). In spatial ICA (sICA), as ICA is usually implemented for fMRI, the blood-oxygen-level dependent (BOLD) contrast image volume is assumed to be a linear mixture of spatially independent components which may originate from different sources. The time courses and spatial maps of the components can be decomposed by estimating the mixing matrix using a variety of algorithms (Hyvärinen and Oja, 2000). Methods have also been proposed to extend ICA to analyze multi-subject fMRI data (Calhoun et al., 2001b; Svensen et al., 2002; Esposito et al., 2005; Beckmann and Smith, 2005b). Schmithorst and Holland (2004b) compared three methods of group ICA analysis (across-subject averaging, subject-wise concatenation, and row-wise concatenation) and concluded that the subject-wise concatenation approach proposed by Calhoun et al. (2001b) provided the best overall performance among the three approaches. This method has been used in studies of visual perception (Calhoun et al., 2001b), numerical processing for complex math operations (Schmithorst and Brown, 2004a), narrative comprehension (Schmithorst et al., 2006), and complex natural environment (Malinen et al., 2007).

We performed a group ICA analysis on fMRI data of two word generation tasks from fourteen healthy subjects. We focused on the similar activation patterns revealed by both language tasks since they represented the brain regions that were important across both paradigms. To this end, we used similarity analysis on the component spatial maps derived from two tasks to identify the common components of interest (CCOIs); among the CCOIs we identified the language-specific components.

In addition, since any single language task is unlikely to engage all aspects of language function, we investigated strategies of combining results *across* different tasks. First, in order to maximize the sensitivity of the procedure, we performed a union analysis on the language-specific CCOIs across tasks. Second, for the purpose of identifying the likely essential language areas, we performed a conjunction analysis (intersection) on the language-specific CCOIs. We then compared the ICA results with the conventional GLM method. Finally, fMRI data from one brain tumor patient was analyzed for comparison of ICA and GLM methods as potential pre-surgical planning tools.

MATERIALS AND METHODS

Subjects and functional MRI

The protocol was approved by the Partner's Institutional Review Board. Fourteen right-handed native English speaking healthy subjects participated in the group study (7 female, mean age = 27.6 ± 9.5 years, range 21–53 years). One right-handed brain tumor patient (male, 30 years old, with anaplastic oligodendroglioma WHO Grade III tumor located in the left frontal lobe) was also studied. All subjects provided written informed consent.

MR images were obtained using a 3.0 Tesla GE Signa system (General Electronic, Milwaukee, WI, USA). A single-shot gradient-echo echo-planar imaging (EPI) was used to acquire BOLD functional images (TR = 2000 ms, TE = 40 ms, flip angle = 90°, FOV = 24 cm, acquisition matrix = 64 × 64, slice gap = 0 mm, voxel size = 3.75 × 3.75 × 5 mm^3). In each image volume, 28 axial slices were acquired using ascending interleaved scanning sequence. Whole brain T1-weighted axial 3D-SPGR (spoiled gradient recalled) MR images (TR = 7500 ms, TE = 30 ms, flip angle = 20°, matrix = 512 × 512, 176 slices, voxel size = 0.5 × 0.5 × 1 mm^3) were also acquired for subsequent overlay of functional activation maps. High-resolution T2-weighted gradient-echo MR images (TR = 8000 ms, TE = 98 ms, flip angle = 90°, matrix = 512 × 512, 93 slices, voxel size = 0.5 × 0.5 × 1.5 mm^3) were acquired for the patient data in order to demonstrate the surgical pathology.

Subjects performed two non-vocalized (silent) word generation tasks: antonym generation (AG), and verbal fluency (VF). The tasks were implemented as blocked designs consisting of six pairs of alternating task and rest blocks with 20 sec block duration, lasting 4 min 10 sec (including a 10 sec pre-stimulus period excluded from analysis to allow stabilization of the BOLD signal). Stimuli for both tasks were presented visually through MR-compatible video goggles (Resonance Technology, Los Angeles, CA, USA). In the AG task, eight words were presented to the subjects sequentially during each task block. Each word was shown for 2000 ms with a 500 ms inter-stimulus-interval (ISI). Subjects were instructed to think of the antonym of the presented word without speaking aloud. In the VF task, a single letter was presented for the entire duration of each task block (20 sec). Subjects were asked to generate covertly as many words as possible beginning with the presented letter. During the rest blocks of both tasks, subjects were asked to relax and look at a crosshair shown in the center of the visual field.

Data pre-processing

FMRI data from the two language tasks were analyzed separately. We used the SPM2 software package (Statistical Parametric Mapping, Wellcome Department of Cognitive Neurology, London, UK) to perform slice-timing correction to account for the difference in image acquisition time between slices; and then motion correction by realigning the functional images to the first volume of each task. Spatial normalization to Montreal Neurological Institute (MNI) space was performed subsequently on the healthy subjects' data, re-sampling all functional

images to $3 \times 3 \times 3$ mm^3 voxels by trilinear interpolation (resulting dimension = $53 \times 63 \times 46$). Spatial smoothing was not applied to the images.

Group ICA analysis of healthy subjects' data

We applied the subject-wise concatenation approach of group ICA analysis (Calhoun et al., 2001b) using the GIFT software package (Group ICA of fMRI Toolbox, Olin Neuropsychiatry Research Center, Hartford, CT, USA). Prior to the ICA procedure, two data reduction steps were performed using principal component analysis (PCA) to reduce data dimension and thus reduce the computational load. The number of independent components (ICs) was estimated for each subject separately using minimum description length (MDL) criteria (Li et al., 2007). The number of ICs was estimated as 29 ± 4 (mean ± SD across subjects) for the AG task, and 31 ± 5 for the VF task. We chose to use the maximum number among all subjects (39 for the AG task, and 41 for the VF task) in the first data reduction step, due to the concern of under-fitting individual subject data and thus losing important information. Therefore the AG task data of each subject was reduced to 39 time points (from 120 time points of the original data set), and the VF task data of each subject was reduced to 41 time points. In the second data reduction step, we did not use MDL, instead we explored different numbers of ICs, e.g., the mean or maximum number of ICs among all subjects. With the concern of under-fitting individual subject data, and for the purpose of accommodating the variability of artifactual components across subjects, we also tested a higher number of ICs (i.e., 50). Among all experiments of different numbers of ICs, 50 seemed to generate plausible results without over-fitting the activation patterns. Therefore in the second data reduction step for each task, the reduced data of each subject were concatenated and further reduced to 50 time points. It is worth mentioning that MDL is only one possible indicative measure of a reasonable number of dimensions to keep, and cannot be considered a rule.

The reduced data were then decomposed into "group independent components" by the Infomax ICA algorithm (Bell and Sejnowski, 1995). Each group IC had a spatial map and a corresponding temporal activation profile (time course). Subsequently single subject IC spatial maps and time courses were back-reconstructed from group ICs based on the results from data reduction steps, and then scaled to z-scores.

Selection of common components of interest (CCOIs)

In order to identify common activations by both tasks, we performed a spatial similarity analysis on the components across tasks. We designated as $\boldsymbol{r}_{AiVj}$ the spatial correlation coefficient between the mean z-score map (averaged across subjects) of the $\boldsymbol{i}^{th}$ IC of the AG task and the mean z-score map of the $\boldsymbol{j}^{th}$ IC of the VF task, using Pearson's correlation equation:

$$r_{\mathrm{AiVj}} = \frac{\sum_{m} A_{im} V_{jm}}{N}, i, j = 1, 2, \ldots 50, \qquad \text{(Equation 1)}$$

where $\boldsymbol{A}_{im}$ and $\boldsymbol{V}_{jm}$ are the intensity of voxel $\boldsymbol{m}$ in the $\boldsymbol{i}^{th}$ IC map of the AG task and the $\boldsymbol{j}^{th}$ IC map of the VF task respectively, and $\boldsymbol{N}$ is the number of voxels in the spatial maps. Then the similarity measure of the $\boldsymbol{i}^{th}$ IC of the AG task is:

$$r_{Ai} = \max_{j} \{r_{AiVj}\}, j = 1, 2, \ldots 50 . \qquad \text{(Equation 2)}$$

Similarly $\boldsymbol{r}_{ViAj}$ and $\boldsymbol{r}_{Vi}$ were calculated for each IC of the VF task as well. Then we specified an arbitrary threshold of the similarity measure $\boldsymbol{r} = 0.5$ to define the common components across tasks, yielding pairs of ICs with highly similar spatial maps.

There were 30 ICs of the AG task whose $\boldsymbol{r}_{Ai}$ was higher than 0.5 with its counterpart IC from the VF task, and 29 ICs of the VF task whose $\boldsymbol{r}_{Vi}$ was higher than 0.5 with its counterpart IC

from the AG task. Among these components, 29 pairs of ICs confirmed their mutual similarity. A special case was that one IC of the VF task had two counterpart ICs from the AG task. We subsequently focused our analysis on these common components and visually inspected their spatial maps. We excluded the components that highlighted veins, the ventricular system, or other non-cortical regions. Finally, for each remaining common component of interest (CCOI), a random-effects (RFX) analysis was performed on the back-reconstructed individual subjects' maps by a one-sample ***t*** test. The ***t*** maps were thresholded at $|t| = 3.85$ ($p < 0.001$, degrees of freedom (df) = 13).

GLM analysis of healthy subjects' data

For comparison purposes, the pre-processed data sets were submitted to SPM2 for conventional analysis based on the GLM method. In the first-level single subject analysis, an estimate of the canonical hemodynamic response function (HRF) was used as the basis function, and only task conditions were explicitly modeled. Then a second-level RFX analysis was performed by one-sample ***t*** test on the contrast images derived from the single subject analyses. The ***t*** maps were thresholded at $t = 3.85$ ($p < 0.001$, df = 13) in order to be comparable with the ICA results.

Voxel count in the putative language areas

To facilitate a quantitative comparison between the ICA-derived maps and the GLM maps in terms of the number of supra-threshold voxels identified in the putative language areas, two region of interest (ROI) images were generated for Broca's and Wernicke's areas respectively (shown in Figure 1), based on the Talairach Daemon database (Talairach and Tournoux, 1988), using WFU Pick Atlas software (version 1.04, Department of Radiology, Wake Forest University, Winston-Salem, NC, USA) (Lancaster et al., 1997,2000; Maldian et al, 2003). The ROI for Broca's area consisted of Brodmann areas (BAs) 44 and 45 in the left hemisphere; and the ROI for Wernicke's area consisted of the posterior half of the left superior temporal gyrus. Then the number of supra-threshold voxels that were located within the ROI images was counted for each map, using Brain Imaging Tools (BIT, Gabrieli Lab, Department of Brain and Cognitive Sciences, Massachusetts Institute of Technology, Cambridge, MA, USA).

Data analysis of one tumor patient's data

We performed single subject analysis using both ICA and GLM methods on the patient's pre-processed data (after slice-timing and motion correction procedures). For the ICA method, the number of components was estimated as 60 for the AG task, and 55 for the VF task, using MDL, and PCA was used to reduce the data dimension. Then for each task, the Infomax ICA algorithm was applied to separate the data into independent components, whose spatial maps were scaled to z-scores and thresholded at $|z| = 2$. A similarity analysis was applied on the spatial maps across both tasks to select components of interest. In the GLM method, first-level analysis was applied to each task, and the activation maps were thresholded at $t = 2.35$ ($p < 0.01$, uncorrected, df = 133) for the AG task, and $t = 1.66$ ($p < 0.05$, uncorrected, df = 118) for the VF task. The ***t*** threshold was chosen relatively lenient for better visualization of the activation clusters.

RESULTS

Language-specific CCOIs

Out of the 29 pairs of common components across both tasks, and one additional component of the AG task, there were 5 pairs showing signals from the veins, 2 pairs showing signals in the ventricular system, 5 pairs showing signals in the cerebellum, and 3 pairs showing signals in the brainstem. These 15 pairs of common components were excluded from further analysis.

For the remaining 14 pairs of CCOIs and one additional IC of the AG task, the MNI coordinates of the supra-threshold voxels were submitted to WFU Pick Atlas database to find the corresponding anatomic regions and BAs, using a custom toolbox. Then based on the knowledge of the location of putative language areas in the left frontal and temporal lobes in the right-handed control population, we classified two ICs from the AG task (designated as *ag1* and *ag2*) and one IC from the VF task (designated as *vf1*) as "language-specific" CCOIs (note that both *ag1* and *ag2* had the same counterpart IC from the VF task, which is *vf1*, their similarity measures are listed in Table 1). The spatial maps of these language-specific CCOIs are shown in Figure 1, and their activation regions are listed in Table 1. For the AG task, *ag1* demonstrates significant activation in the left inferior/middle frontal gyrus; *ag2* shows activation in the left superior/middle temporal gyrus and superior/inferior frontal gyrus. For the VF task, *vf1* demonstrated robust activations mainly in the left frontal lobe (especially the inferior/middle/superior frontal gyrus), with some activation in the lentiform nucleus and caudate.

The time courses of the language-specific CCOIs are plotted in Figure 2 for individual subjects, as well as the mean time course across subjects (shown in red), and the reference function generated by convolving the design matrix boxcar with an estimate of the HRF (shown in blue). The correlation coefficients between IC time course and the reference function are 0.48 ± 0.18 (mean ± SD), 0.53 ± 0.19, and 0.68 ± 0.13 for *ag1*, *ag2*, and *vf1* respectively (all $p < 0.0001$). We also ranked the 50 separated components based on their temporal correlation with the reference function. The results indicated that *ag1* and *ag2* ranked the fifth and the second among ICs of the AG task, and *vf1* was the most task-related IC of the VF task.

Comparison of language-specific CCOIs maps with GLM maps

The activation maps of GLM group analysis are shown in Figure 1, for comparison with the ICA-derived language-specific maps. The results of quantitative comparison between language-specific CCOI maps and the GLM maps are listed in Table 2, showing the number of supra-threshold voxels that were located in the putative language ROIs. For the AG task, the activations of *ag1* were mainly located in Broca's area, and those of *ag2* were mainly located in Wernicke's area. The combination of these two components showed substantially more voxels (n = 108) in Wernicke's area compared with the GLM maps (n = 5), although the number of voxels in Broca's area (n = 138) is less than that in the GLM maps (n = 176). For the VF task, there are twice as many voxels in Broca's area in *vf1* maps (n = 185) than in the GLM maps (n = 91). Compared with the GLM results, the language-specific CCOIs showed a greater proportion of total activated voxels in the thresholded maps that were located within the putative language ROIs, indicating that the ICA-derived maps are more specific to the language areas with less activation in the non-language-specific region.

We have further investigated the GLM results of the areas that were identified by the ICA method but not shown in the GLM maps at the same group statistical significance level ($p < 0.001$, t-threshold = 3.85). For the AG task, the ICA-derived maps identified 103 supra-threshold voxels that were not identified by the GLM method within the Wernicke's ROI. The t-score of those voxels is 1.19 ± 1.24 (mean ± SD). For the VF task, the t-score of the voxels in the Broca's ROI that were not identified by the GLM method is 2.61 ± 0.75 (n = 94). As for the Wernicke's ROI, there are 5 voxels identified by the ICA method but not shown in the GLM maps ($t_{max} = 0.91$, $t_{min} = -3.88$).

Analysis across both tasks

The results from both tasks were combined in two ways. First, in an effort to increase the sensitivity of language mapping, we performed a union analysis on the thresholded maps of the ICA-derived language-specific CCOIs. The union maps consisted of activations in the maps

of any component among *ag1*, *ag2*, and *vf1*, and are shown in Figure 1. Second, to identify the likely essential language regions, we performed a conjunction analysis similar to the approach for multi-task fMRI analysis based on the GLM method (Nichols et al., 2005). To this end, the language regions identified by the AG task were first represented by the union maps of *ag1* and *ag2*, then the intersection of this union map and *vf1* maps were generated for the conjunction maps, which are shown in Figure 1. For comparison purposes, we also performed both union and conjunction analyses to combine the GLM results from both tasks (Figure 1). The voxel count results in each map are listed in Table 1. The results of both union and conjunction analyses indicated that the ICA method identified more activated voxels in the putative language areas than the GLM method. The ICA-derived conjunction maps identified a greater proportion of overall activated voxels in the language ROIs, indicating more language-specificity compared with the GLM-derived conjunction maps.

Non-language-specific CCOIs identified by ICA

In addition to the language-specific CCOIs, there were 13 pairs of non-language-specific CCOIs identified by both tasks. We classified these components into three categories based on their activation regions. Their thresholded ***t*** maps are shown in Figure 3 (for AG task). The anatomical regions and BAs of their activations, the spatial similarity measures across tasks, and the correlation coefficients between their time courses and the reference function are listed in Table 1.

The first category has one pair of CCOIs, with activations primarily in the perisylvian region in bilateral inferior/middle frontal gyrus, and bilateral superior/middle temporal gyrus. The second category consists of 6 pairs of CCOIs, with activations in the motor and sensory cortical areas. The third category consists of 6 pairs of CCOIs, with activations in different parts of parietal lobule, precuneus, and cingulate.

Results of single patient's data

Figure 4 shows the ICA and GLM results of the brain tumor patient's data. The similarity analysis identified two language-specific components from the AG task, and one from the VF task. The red component of the AG task resembles the GLM activation maps, showing activations in the left frontal and temporal lobes, and in the lateral visual areas. The green component shows significant activations in Broca's area. For the VF task, the ICA-derived maps and the GLM maps identify similar activated areas, while ICA maps have less extraneous activations in the non-language-specific region. Temporal correlation analysis indicated that these language-specific components are the most task-related components among the separated ICs for each task ($r = 0.54$ and 0.35 for the red and green components of the AG task, $r = 0.81$ for the language component of the VF task, all $\boldsymbol{p} < 0.0001$).

DISCUSSION

In this study, we performed group ICA analysis on fMRI data from two language tasks in fourteen healthy subjects to assess the overall performance of ICA with regards to improving the sensitivity and specificity of language mapping. We applied a novel strategy of choosing components of interest based on spatial similarity of the components across different tasks. Among the identified common components, two language-specific components were identified for the AG task and one for the VF task. We subsequently compared the ICA-derived language maps with the GLM results at the same group statistical significance level. In general, the language-specific CCOIs identified more activated voxels in the putative language areas, indicating the potential advantage of ICA in reducing type II error. Furthermore, the union maps derived by the ICA method identified more activated voxels in the putative language

areas than that of the GLM method, indicating an increase in the sensitivity of language mapping.

In addition to the language-specific CCOIs, several non-language-specific CCOIs were also identified. This finding confirmed the usefulness of ICA to isolate signals from other areas that may participate in language tasks, and therefore provide activation maps more specific to the language function *per se*. Furthermore, in an effort to reveal the areas likely essential to the language processing, the conjunction maps derived by the ICA method identified a greater proportion of activated voxels in the putative language areas than that of the GLM method, and therefore more specific to language function.

The results of one brain tumor patient's data are promising regarding the application of ICA as a complementary approach to the conventional GLM method for pre-surgical language mapping. In the AG task, besides one component that was very similar to the GLM results, an additional component was identified with significant activations in Broca's area. In the VF task, compared with the GLM maps, the ICA-derived language maps were more specific to the language areas, showing less extraneous activations elsewhere.

Selection of components of interest in ICA

ICA has proven to be an effective method for detecting spatially independent features of fMRI data without *a priori* assumptions about the time course of different brain processes. A practical challenge for the ICA technique is in the objective selection of the components that are of interest for a given application. Methods have been proposed for this purpose based on spatial, temporal, and spectral criteria (McKeown et al., 1998; Calhoun et al., 2001b; Moritz et al., 2003). In this study, we proposed a strategy for identifying components of interest based on a similarity analysis on the components' spatial maps across different language tasks. The underlying rationale is that the highly similar components revealed by both tasks potentially represent activation patterns that are of interest. Calhoun et al. (2004) used a method for comparing group ICA results by both within-group and between-group similarity analysis, which focused on the components' time courses instead. In our study, we did not rely on the ICs' temporal behavior to select components of interest; rather we depended on their spatial patterns. The advantage of this strategy is that we could identify language associated activations whose temporal behaviors differ from the task timing.

In our study, the spatial maps of the selected common components were then visually inspected, and the components that presumably originated from non-cortical areas (e.g., veins, ventricular system, cerebellum, and brainstem) were excluded from further analysis. Among the remaining CCOIs, we identified the components specific to the language function based on the location of the putative language areas and leftward asymmetry of language activation pattern in a right-handed control population (Binder et al., 1997c).

It is worth mentioning that the proposed similarity analysis can be used to select common components from two tasks. In cases with more than two decompositions, clustering techniques or similar tools are necessary (Esposito et al., 2005; van de Ven et al., 2007).

Language-specific CCOIs

The activated areas identified by the language-specific CCOIs support the hypothesis that brain regions involved in language processing extend well beyond the areas in the classical model (Binder et al., 1997c). Besides Broca's area in the left inferior/middle frontal gyrus (i.e., BAs 44 and 45) that has been linked to both word production and perception (Binder et al., 1997a; Price et al., 1998), and Wernicke's area in the left superior temporal gyrus (i.e., BA 22) that is traditionally related to word comprehension (Cabeza and Nyberg, 2000), a variety of regions

in the left superior/medial frontal gyrus, and the left inferior/middle temporal gyrus were also included in the ICA-derived language maps (see Table 1). Temporal correlation analysis indicated that the language-specific CCOIs were among the most task-related components.

It is interesting to note that there were two language-specific components found from the AG task while only one found from the VF task. *Ag1* was mainly in the left frontal lobe, *ag2* was mainly in the left temporal lobe, whereas *vf1* showed significant activation in the left frontal lobe with only minor activation in the left temporal lobe. This observation may be due to the different cognitive demands of the two tasks. During the antonym generation task, subjects were presented a series of word stimuli, which might require more comprehension at linguistic-semantic and phonological levels, compared with the verbal fluency task in which subjects were presented only one letter as the stimulus cue, which likely requires less linguistic decoding. Therefore, the signals isolated in the temporal lobe (revealed by *ag2*) may be related to the language comprehension that occurs more consistently during the AG task. Under this hypothesis, it is interesting to note that the ICA approach is able to separate the linguistic decoding from the linguistic encoding aspects of language. This separation effect was demonstrated in the single patient data as well. Therefore different tasks, and different combinations of tasks, could be investigated for their usefulness in identifying anatomic substrates underlying various aspects of language processing.

Comparison of ICA and GLM results

Results from group ICA and GLM analyses have been compared in recent studies. Goebel et al. (2006) compared self-organizing group ICA (Esposito et al., 2005) with GLM on a sentence repetition task using fMRI, and concluded that group ICA provided a functional connectivity model by separating different patterns from the data. In another study that used subject-wise concatenation group ICA (Calhoun et al., 2001b) on a series of complex natural environment (Malinen et al., 2007), it was found that the GLM method only revealed sub-areas of the ICA-revealed activations.

In this study, comparison between group ICA and GLM analyses was focused on the activations in the putative language areas from word generation tasks. With the GLM method, approaches have been used to limit type I error associated with multiple comparisons, e.g., Bonferroni correction (Maxwell and Delaney, 1990), random field theory (RFT, Worsley et al., 1996), and false discovery rate (FDR, Benjamini and Hochberg, 1995). However adjustments to control type I error are at the expense of type II error, which is failing to obtain statistical significance when the effects are genuinely present (Loring et al., 2002). For pre-surgical language mapping, type II error is more relevant since it may result in falsely underestimating the extent of critical language cortex and thus resulting in an underestimate of potential surgical risk to language function. In our study, the majority of voxels in the putative language areas that were missed by the GLM method had *t*-scores substantially lower than the chosen threshold, suggesting that their temporal behaviors correlated poorly with the task timing. This can explain why the inferential GLM method failed to identify those areas. Therefore as a complementary method to GLM, ICA can be used to detect activations where the hemodynamic response differs from the model, thus reducing type II error.

Visual inspection of the language maps derived by the ICA and GLM methods indicated that ICA-derived maps were more specific to the language function. This observation is confirmed by the voxel count results demonstrating that a greater proportion of the activated voxels are within the language ROIs in the ICA maps than in the GLM maps. The GLM maps incorporate activations in the regions similar to those in the ICA-derived non-language-specific components (e.g., bilateral activations of the perisylvian, motor, visual, and parietal regions). With the GLM method, approaches have been explored to identify the brain regions involved in specific cognitive processes, e.g., factorial designs, cognitive subtraction, and cognitive

conjunction (Petersen et al., 1990; Price and Friston, 1997; Price et al., 1997). However, these approaches require the implementation of strictly complementary behavioral task conditions, which may be difficult to design, complicated for subjects, particularly patients, to perform, and may generate results that are not straightforward to interpret (Price et al., 1997). Additionally, such task-centered approaches to narrowing the identified language areas may be vulnerable to variability between subjects and approaches, and may also lead to less robust activations in the putative language areas. As such, the advantage of ICA is allowing the decomposition of comprehensive activation maps into distinct components that could be individually assessed with regards to their participation in language processing.

Therefore, in contrast to the approaches using GLM to control type I error of the null hypothesis of “no activation”, and the design strategies using GLM to identify brain regions specific to a cognitive process, ICA offers a complementary and direct investigation into the null hypothesis of “no activation” (by separating noise components), as well as the alternative hypothesis of language-specific vs. non-language-specific activations.

A difficulty encountered with ICA is that the separated components are not always easy to interpret since ICA is a purely exploratory technique. Therefore the GLM maps could be used as a template to help guide the interpretation of components. The advantage of a confirmatory method like GLM is that it provides an integrated picture of all the task-related areas, thus allowing investigators to view all task-related activations together and form their own interpretation of the results. Combining the results from both the confirmatory GLM and the exploratory ICA methods may offer a more complete description of the brain activations associated with language task performance, particularly useful for the specific application of pre-surgical mapping.

The ICA-derived maps showed smoother activations than the analogous GLM maps, indicating that the components from multiple subjects can be well summarized at the group level even without spatial smoothing. This finding can be explained by the fact that the ICA components are made of linear combination of voxels (linear multivariate approach) while the GLM is a linear univariate approach. As a further improvement of ICA by taking into account its linear multivariate property, Formisano et al. (2004) proposed a cortex-based ICA technique (cbICA), restricting the decomposition to the “cortical” sub-region of the matrix, where the resulting component maps are linear combination of voxels laying on a distributed anatomical structure (e.g., cortex). However for clinical applications where the anatomy might be distorted by the lesion, this cortex-based approach should be used with special caution.

Combining different language tasks

In this study, we performed both union and conjunction analyses to combine two language tasks. The purpose of union analysis is to capture activations in the language areas by either task, thus to increase the sensitivity of language mapping. The purpose of conjunction analysis is to capture activation areas that are more likely to be essential for language function, by exclusion of the areas that possibly only participate in, but are not essential to language. These two combination analyses are valuable for pre-surgical language mapping, since the surgeon wishes to have a language map that is both sensitive and specific, in order to identify those brain regions critical for language function so that they may be avoided during the resection, as well as to maximize resection.

Non-language-specific CCOIs

The ICA-derived non-language-specific CCOIs are likely to represent other brain areas that nevertheless are involved in performance of the word generation tasks, although some of them were not highly correlated with the task timing (see Table 1).

The component in category I shows bilateral activation in the perisylvian region, mainly in the inferior frontal gyrus (BA 47) and superior temporal gyrus. BA 47 in the left inferior frontal gyrus has been associated with semantic/syntactic processing (Poldrack et al., 1999). More recently, left BA 47 and its right hemisphere homologue has been speculated to "constitute a modality-independent brain area that organizes structural units in the perceptual stream to create larger, meaningful representation" (Levitin and Menon, 2003). In our study, although this component was not classified as language-specific mainly due to its symmetric activation pattern, we propose that the identified regions may represent brain areas involved in perceptual organization in the language task.

The components in category II represent bilateral activations in the motor and sensory areas. The activations in the primary motor and pre-motor areas are consistent with the findings by Rueckert et al. (1994) in a silent verbal fluency task. The activations in the medial and lateral visual areas, auditory system, and sensory-motor system are consistent with the resting-state patterns reported by Beckmann et al. (2005a).

The components in category III show bilateral activations in different parts of parietal lobule, precuneus, and cingulate. It is interesting to note that the activations in these areas in the left hemisphere have been reported regarding language processing networks (Binder et al., 1997a; 1997c; Levin et al., 1991; Price et al., 1998), however, the bilateral activation pattern identified in this study has not been previously reported.

ICA analysis for single patient's data

In the analysis of one brain tumor patient's data, we applied spatial similarity analysis across tasks to select components of interest, as in the group study. In the AG task, besides one component that resembled the activated areas in the GLM maps, another component (shown in green in Figure 4) demonstrated significant activations in Broca's area. Temporal correlation analysis indicated that this component was poorly correlated with the reference function ($\boldsymbol{r}$ = 0.35, $\boldsymbol{p} < 0.0001$). This observation may explain why the GLM method failed to identify activations in this region, thus resulting in type II error. In the VF task, ICA-derived language maps were similar to the GLM maps, however, ICA maps were less noisy and more specific to the language areas. Our results indicate that ICA-derived maps could be complementary to the GLM maps, especially when GLM fails to identify language activations even at a low statistical significance level. Furthermore, selecting components of interest based on spatial similarity across tasks of the same function might be more useful in cases where the hemodynamic response is difficult to predict, for example, during complicated tasks (e.g., event-related paradigms), or for patients' data.

In a report that compared ICA and hypothesis-driven methods for clinical fMRI tasks (Quigley et al., 2002), it was observed that ICA mapped the language areas less robustly than the conventional regression analysis, which is in contrary to our results of the single patient's data. They postulated that their finding might be due to the separation of language activations into multiple components, and the lack of uniformity of the BOLD signal-to-noise ratio (SNR) across the brain.

Our study on a group of healthy subjects and one brain tumor patient confirmed the possible role of ICA in improving the sensitivity and specificity of fMRI language mapping. Our results suggest that the ICA method may be fruitfully applied as a complementary tool to the GLM method for pre-surgical planning. Further study on single subject/patient language fMRI data, as well as the investigation of optimal task and task combinations will be needed so that this technique may become most clinically useful.

ACKNOWLEDGMENTS

This work is supported by NIH K08 NS048063, NIH-NCRR U41 RR019703, and The Brain Science Foundation. We thank Dr. Susan Whitfield-Gabrieli and Dr. Lauren O'Donnell for their great help and suggestions on this work. We are especially grateful to the anonymous reviewers for their valuable comments.

REFERENCES

Bell AJ, Sejnowski TJ. An information-maximization approach to blind separation and blind deconvolution. Neural Comput 1995;7:1129–1159. [PubMed: 7584893]

Beckmann CF, DeLuca M, Devlin JT, Smith SM. Investigations into resting-state connectivity using independent component analysis. Phil. Trans. R. Soc. B 2005a;360:1001–1013. [PubMed: 16087444]

Beckmann CF, Smith SM. Tensorial extensions of independent component analysis for multisubject FMRI analysis. Neuroimage 2005b;25:294–311. [PubMed: 15734364]

Benjamini Y, Hochberg Y. Controlling the false discovery rate: a practical and powerful approach to multiple testing. J. R. Statist. Soc., Ser. B 1995;57:289–300.

Binder JR, Swanson SJ, Hammeke TA, Morris GL, Mueller WM, Fischer M, Benbadis S, Frost JA, Rao SM, Haughton VM. Determination of language dominance using functional MRI: a comparison with the Wada test. Neurology 1996;46:978–984. [PubMed: 8780076]

Binder JR. Neuroanatomy of language processing studied with functional MRI. Clin. Neurosci 1997a; 4:87–94. [PubMed: 9059758]

Binder JR. Functional magnetic resonance imaging: language mapping. Neurosurg. Clin. N. Am 1997b; 8:383–392. [PubMed: 9188545]

Binder JR, Frost JA, Hammeke TA, Cox RW, Rao SM, Prieto T. Human brain language areas identified by functional magnetic resonance imaging. J. Neurosci 1997c;17:353–362. [PubMed: 8987760]

Binder, JR. Functional MRI of the language system. In: Moonen, CTW.; Bandettini, PA., editors. Functional MRI. Springer; 2000. p. 407-419.

Bookheimer S. Pre-surgical language mapping with functional magnetic resonance imaging. Neuropsychol. Rev 2007;17:145–155. [PubMed: 17484055]

Brannen JH, Badie B, Moritz CH, Quigley M, Meyerand ME, Haughton VM. Reliability of functional MR imaging with word-generation tasks for mapping Broca's area. AJNR Am. J. Neuroradiol 2001;22:1711–1718. [PubMed: 11673166]

Cabeza R, Nyberg L. Imaging cognition II: an empirical review of 275 PET and fMRI studies. J. Cogn. Neurosci 2000;12:1–47. [PubMed: 10769304]

Calhoun VD, Adali T, McGinty VB, Pekar JJ, Watson TD, Pearlson GD. fMRI activation in a visual-perception task: network of areas detected using the general linear model and independent components analysis. Neuroimage 2001a;14:1080–1088. [PubMed: 11697939]

Calhoun VD, Adali T, Pearlson GD, Pekar JJ. A method for making group inferences from functional MRI data using independent component analysis. Hum. Brain Mapp 2001b;14:140–151. [PubMed: 11559959]

Calhoun VD, Adali T, Pekar JJ. A method for comparing group fMRI data using independent component analysis: application to visual, motor and visuomotor tasks. Magn. Reson. Imaging 2004;22:1181–1191. [PubMed: 15607089]

Carpentier A, Pugh KR, Westerveld M, Studholme C, Skrinjar O, Thompson JL, Spencer DD, Constable RT. Functional MRI of language processing: dependence on input modality and temporal lobe epilepsy. Epilepsia 2001;42:1241–1254. [PubMed: 11737158]

Duann J-P, Jung T-P, Kuo W-J, Yeh T-C, Makeig S, Hsieh J-C, Sejnowski TJ. Single-trial variability in event-related BOLD signals. Neuroimage 2002;15:823–835. [PubMed: 11906223]

Esposito F, Scarabino T, Hyvarinen A, Himberg J, Formisano E, Comani S, Tedeschi G, Goebel R, Seifritz E, Salle FD. Independent component analysis of fMRI group studies by self-organizing clustering. Neuroimage 2005;25:193–205. [PubMed: 15734355]

Formisano E, Esposito F, Di Salle F, Goebel R. Cortex-based independent component analysis of fMRI time series. Magn Reson Imaging 2004;22:1493–1504. [PubMed: 15707799]

Friston KJ, Holmes AP, Worsley KJ, Poline J-P, Frith CD, Frackowiak RSJ. Statistical parametric maps in functional imaging: A general linear approach. Hum. Brain Mapp 1995;2:189–210.

Goebel R, Esposito F, Formisano E. Analysis of functional image analysis contest (FIAC) data with brainvoyager QX: From single-subject to cortically aligned group general linear model analysis and self-organizing group independent component analysis. Hum. Brain Mapp 2006;27:392–401. [PubMed: 16596654]

Hyvärinen A, Oja E. Independent component analysis: algorithms and applications. Neural Netw 2000;13:411–430. [PubMed: 10946390]

Lancaster JL, Summerln JL, Rainey L, Freitas CS, Fox PT. The Talairach Daemon, a database server for Talairach Atlas Labels. Neuroimage 1997;5:S633.

Lancaster JL, Woldorff MG, Parsons LM, Liotti M, Freitas CS, Rainey L, Kochunov PV, Nickerson D, Mikiten SA, Fox PT. Automated Talairach atlas labels for functional brain mapping. Hum. Brain Mapp 2000;10:120–131. [PubMed: 10912591]

Levin, HS.; Eisenberg, HM.; Benton, AL. Frontal Lobe Function and Dysfunction. New York: Oxford University Press, Inc.; 1991.

Levitin DJ, Menon V. Musical structure is processed in “language” areas of the brain: a possible role for Brodmann Area 47 in temporal coherence. Neuroimage 2003;20:2142–2152. [PubMed: 14683718]

Li Y-O, Adali T, Calhoun VD. Estimating the number of independent components for functional magnetic resonance imaging data. Hum. Brain Mapp 2007;28:1251–1266. [PubMed: 17274023]

Loring DW, Meador KJ, Allison JD, Pillai JJ, Lavin T, Lee GP, Balan A, Dave V. Now you see it, now you don’t: statistical and methodological consideration in fMRI. Epilepsy Behav 2002;3:539–547. [PubMed: 12609249]

Maldjian JA, Laurienti PJ, Kraft RA, Burdette JH. An automated method for neuroanatomic and cytoarchitectonic atlas-based interrogation of fmri data sets. Neuroimage 2003;19:1233–1239. [PubMed: 12880848]

Malinen S, Hlushchuk Y, Hari R. Towards natural stimulation in fMRI—issues of data analysis. Neuroimage 2007;35:131–139. [PubMed: 17208459]

Maxwell, SE.; Delaney, HD. Designing experiments and analyzing data: a model comparison perspective. Belmont, CA: Wadsworth; 1990.

McKeown MJ, Jung T-P, Makeig S, Brown G, Kindermann SS, Lee T-W, Sejnowski TJ. Spatially independent activity patterns in functional MRI data during the Stroop color-naming task. Proc. Natl. Acad. Sci. USA 1998;95:803–810. [PubMed: 9448244]

Moritz CH, Rogers BP, Meyerand ME. Power spectrum ranked independent component analysis of a periodic fMRI complex motor paradigm. Ham. Brain Mapp 2003;18:111–122.

Nichols T, Brett M, Andersson J, Wager T, Poline J-B. Valid conjunction inference with the minimum statistic. Neuroimage 2005;25:653–660. [PubMed: 15808966]

Petersen SE, Fox PT, Snyder AZ, Raichle ME. Activation of extrastriate and frontal cortical areas by visual words and word-like stimuli. Science 1990;249:1041–1044. [PubMed: 2396097]

Poldrack RA, Wagner AD, Prull MW, Desmond JE, Glover GH, Gabrieli JDE. Functional specialization of semantic and phonological processing in the left inferior prefrontal cortex. Neuroimage 1999;10:15–35. [PubMed: 10385578]

Price CJ, Friston KJ. Cognitive conjunction: A new approach to brain activation experiments. Neuroimage 1997;5:261–270. [PubMed: 9345555]

Price CJ, Moore CJ, Friston KJ. Subtractions, conjunctions, and interactions in experimental design of activation studies. Hum. Brain Mapp 1997;5:264–272.

Price CJ. The functional anatomy of word comprehension and production. Trends Cogn. Sci 1998;2:281–288.

Quigley MA, Haughton VM, Carew J, Cordes D, Moritz CH, Meyerand ME. Comparison of independent component analysis and conventional hypothesis-driven analysis for clinical functional MRI image processing. AJNR Am. J. Neuroradiol 2002;23:49–58. [PubMed: 11827875]

Rueckert L, Appollonio I, Grafman J, Jezzard P, Johnson R Jr. Le Bihan D, Turner R. Magnetic resonance imaging functional activation of left frontal cortex during covert word production. J. Neuroimaing 1994;4:67–70.

Schmithorst VJ, Brown RD. Empirical validation of the triple-code model of numerical processing for complex math operations using functional MRI and group independent component analysis of the mental addition and subtraction of fractions. Neuroimage 2004a;22:1414–1420. [PubMed: 15219612]

Schmithorst VJ, Holland SK. Comparison of three methods for generating group statistical inferences from independent component analysis of functional magnetic resonance imaging data. J. Magn. Reson. Imaging 2004b;19:365–368. [PubMed: 14994306]

Schmithorst VJ, Holland SK, Plante E. Cognitive modules utilized for narrative comprehension in children: A functional magnetic resonance imaging study. Neuroimage 2006;29:254–266. [PubMed: 16109491]

Seifritz E, Esposito F, Hennel F, Mustovic H, Neuhoff JG, Bilecen D, Tedeschi G, Scheffler K, Salle FD. Spatiotemporal pattern of neural processing in the human auditory cortex. Science 2002;297:1706–1708. [PubMed: 12215648]

Stippich C, Rapps N, Dreyhaupt J, Durst A, Kress B, Nenning E, Tronnier VM, Sartor K. Localizing and lateralizing language in patients with brain tumors: feasibility of routine preoperative functional MR imaging in 81 consecutive patients. Radiology 2007;243:828–836. [PubMed: 17517936]

Svensen M, Kruggel F, Benali H. ICA of fMRI group study data. Neuroimage 2002;16:551–563. [PubMed: 12169242]

Talairach, J.; Tournoux, P. Co-planar stereostactic atlas of the human brain. Stuttgart: Thieme; 1988.

Tharin S, Golby A. Functional brain mapping and its application to neurosurgery. Neurosurgery 2007;60:185–201. [PubMed: 17415154]discussion 201–202

van de Ven V, Bledowski C, Prvulovic D, Goebel R, Formisano E, Di Salle F, Linden DE, Esposito F. Visual target modulation of functional connectivity networks revealed by self-organizing group ICA. Hum Brain Mapp. 2007[Epub ahead of print]

Woermann FG, Jokeit H, Luerding R, Freitag H, Schulz R, Guertler S, Okujava M, Wolf P, Tuxhorn I, Ebner A. Language lateralization by Wada test and fMRI in 100 patients with epilepsy. Neurology 2003;61:699–701. [PubMed: 12963768]

Worsley KJ, Marrett S, Neelin P, Vandal AC, Friston KJ, Evans AC. A unified statistical approach for determining significant voxels in images of cerebral activation. Hum. Brain Mapp 1996;4:58–73.

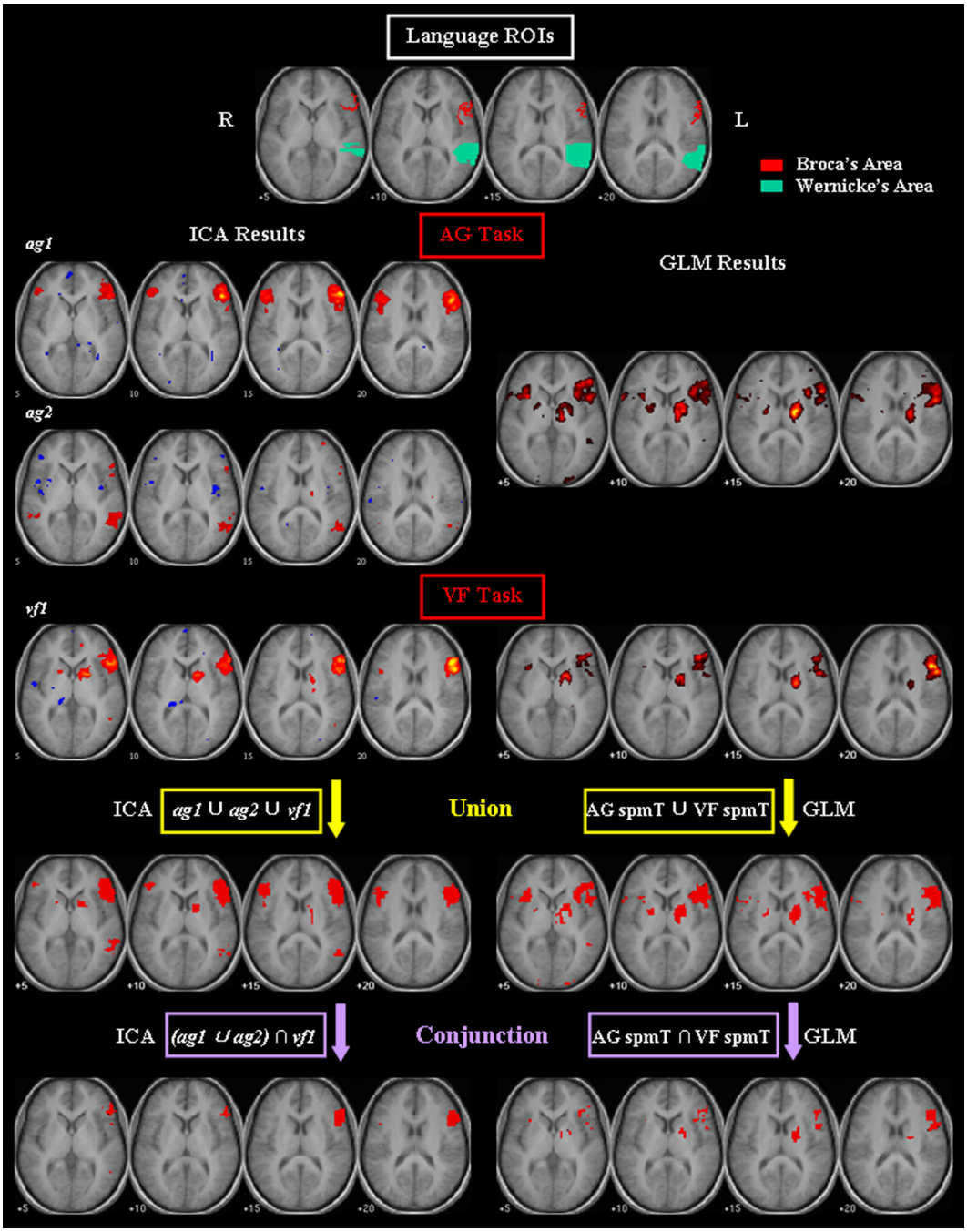

Figure 1.

Comparison of group ICA and GLM analyses of fMRI from antonym generation (AG) and verbal fluency (VF) tasks from healthy subjects. ROI images in the putative language areas (red: Broca's area; green: Wernicke's area) are shown. The thresholded group activation maps of the language-specific CCOIs (*ag1* and *ag2* for the AG task, and *vf1* for the VF task; $|t| = 3.85$) are superimposed on the averaged SPGR images. Results of union and conjunction analyses by ICA and GLM methods are shown in the last two rows.

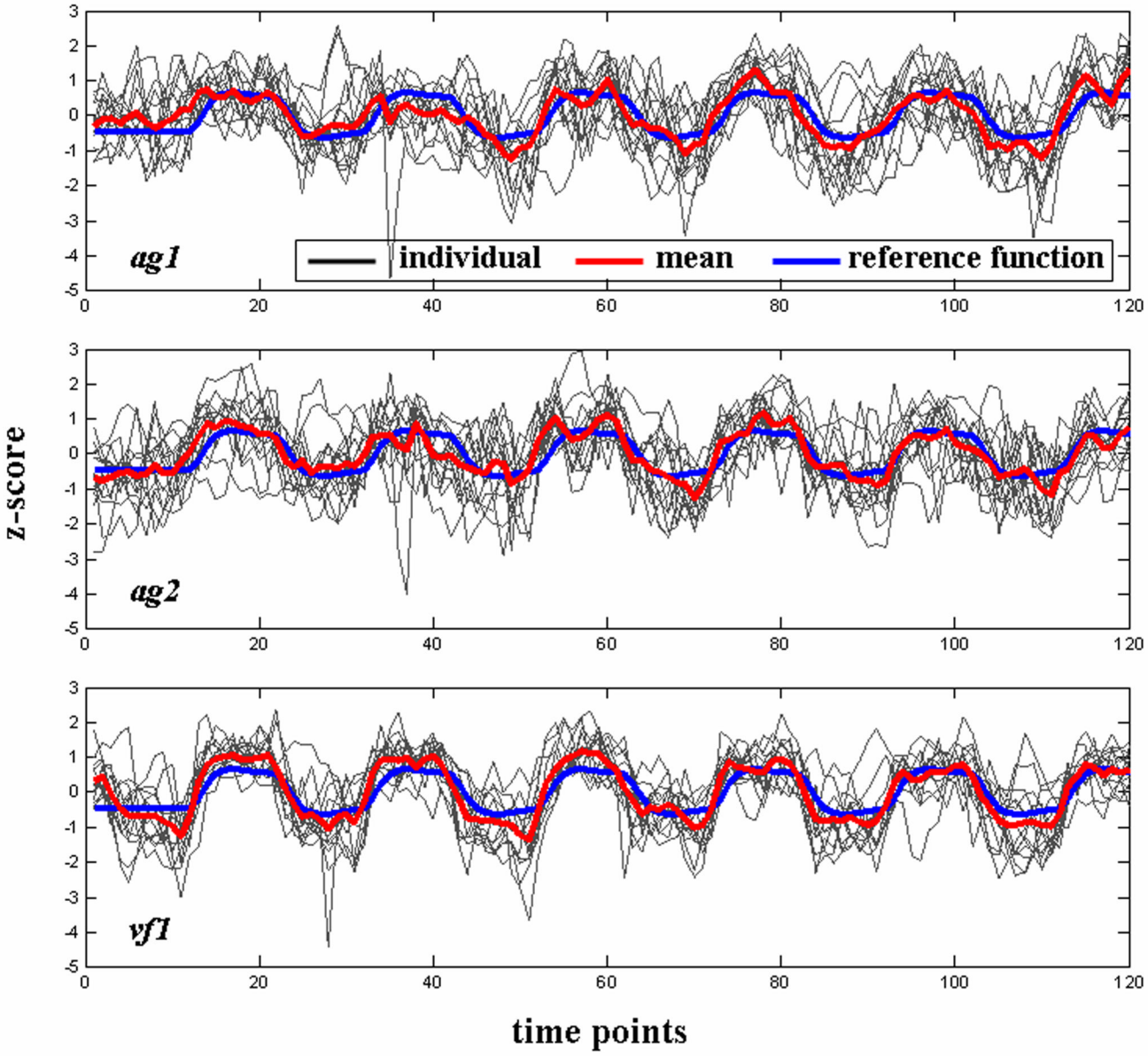

Figure 2.
Time courses of the language-specific CCOIs (plotted for each subject individually). The mean time course averaged across subjects is shown in red, and the reference function is shown in blue. All time courses are scaled to z-scores.

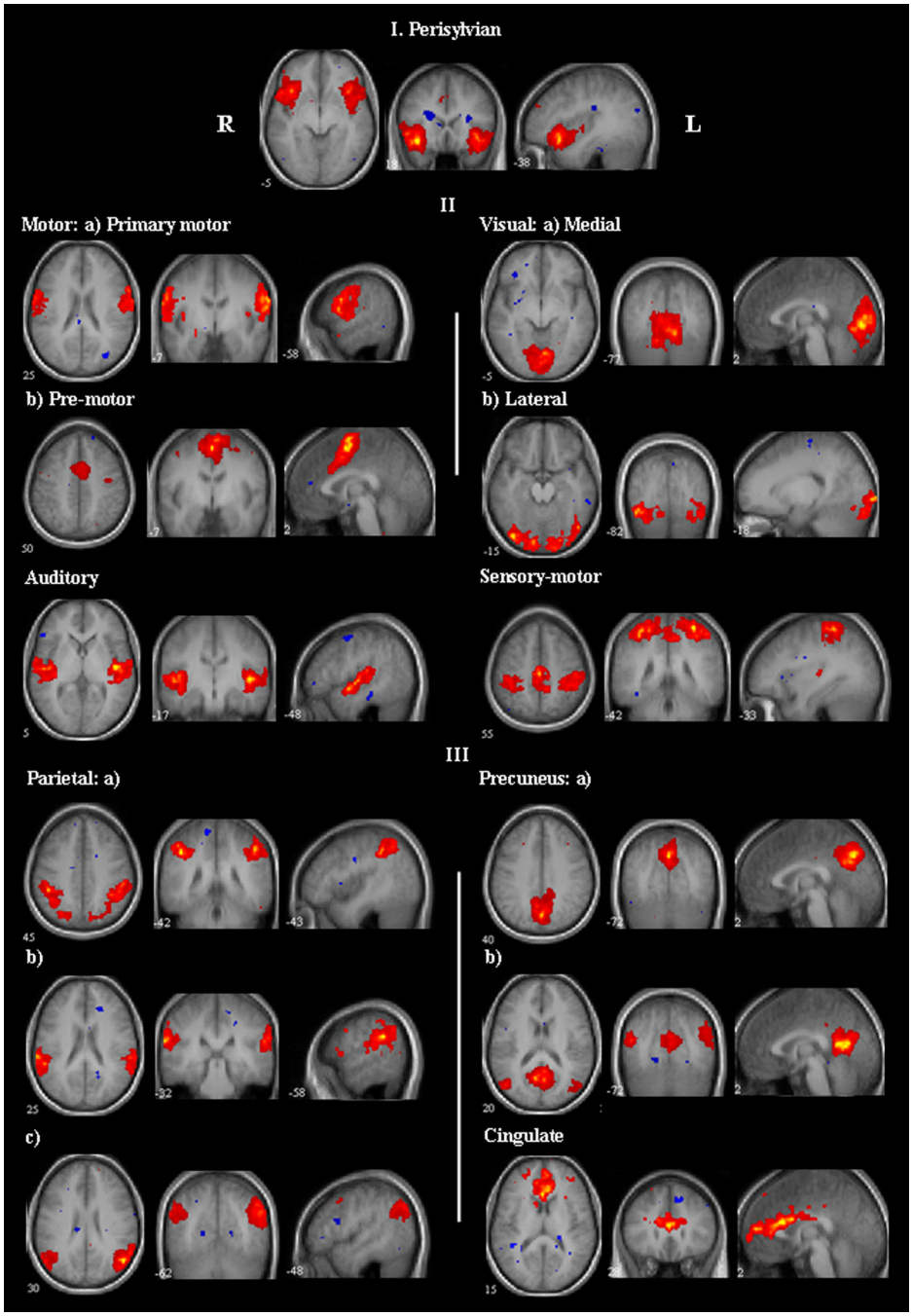

Figure 3.

Group activation maps of the non-language-specific CCOIs identified from the AG task (their counterpart ICs from the VF task have highly similar spatial maps, not shown). The CCOIs are classified into three categories based on their activation regions. Category I: activations in the perisylvian region; category II: activations in the motor and sensory cortical areas; category III: activations in the parietal lobule, precuneus, and cingulate. All maps are thresholded at $|t| = 3.85$.

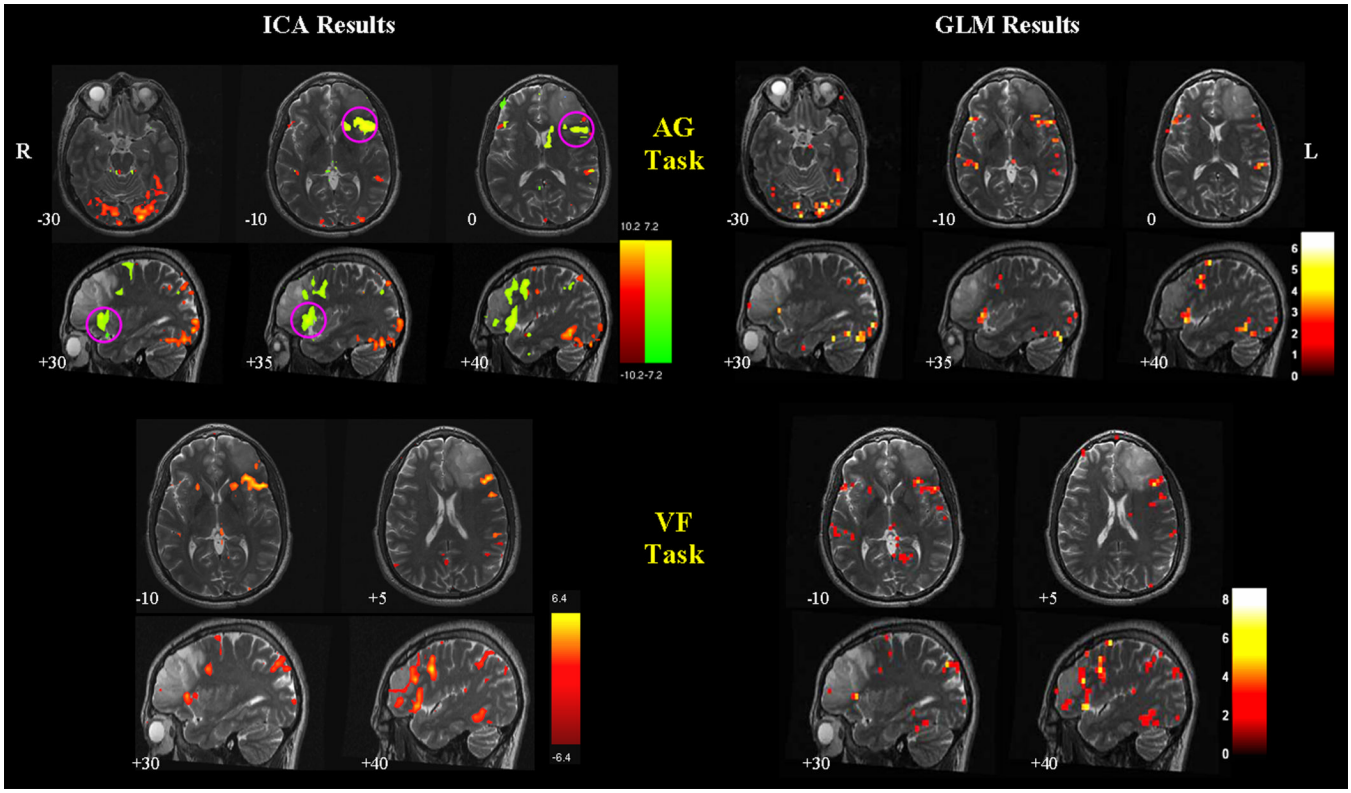

Figure 4.

Comparison of ICA and GLM results of the brain tumor patient's data. Two language-specific components (shown in red and green) are identified from the AG task, and one is identified from the VF task. In the AG task, the red component resembles the activations in the GLM maps. The green component reveals activations in Broca's areas that were not shown in the GLM maps (highlighted by magenta circles). In the VF task, the ICA and GLM maps are similar, but the GLM maps are noisier with activations in the non-language-specific regions. All ICA component maps are thresholded at $|z| = 2$. GLM maps of the AG task are thresholded at $t = 2.35$ ($p < 0.01$, uncorrected). GLM maps of the VF task are thresholded at a lenient level of $t = 1.66$ ($p < 0.05$, uncorrected) for better visualization of the activations in the language areas. The background structural images are high-resolution T2 images coregistered to the first functional image of the corresponding task.

Table 1

Common components of interest (CCOIs) identified by both AG and VF tasks.

		CCOIs		Activation Region	Brodmann Area (BA)	Similarity Measure (*r*)	Temporal Correlation with Reference Function (*r*)	
							AG	VF
Language-specific CCOIs		*ag1*		Left inferior/middle/superior frontal gyrus, precentral gyrus	6, 9, 44, 45, 46, 47	0.52 (to *vf1*)	0.48 ± 0.18	
		ag2		Left inferior/superior frontal gyrus; left inferior/middle/ superior temporal gyrus	6, 8, 9, 10, 44, 45, 47; 19, 21, 22, 38, 39	0.51 (to *vf1*)	0.53 ± 0.19	
		vf1		Left inferior/middle/superior/ medial frontal gyrus, precentral gyrus; left inferior/middle/ superior temporal gyrus; lentiform nucleus; caudate	6, 8, 9, 10, 44, 45, 46, 47; 19, 20, 21, 22, 38, 39	0.52 (to *ag1*)		0.68 ± 0.13
Non-language-specific CCOIs	**I**	Perisylvian		Inferior/middle frontal gyrus; superior/middle temporal gyrus	47; 38	0.66	0.40 ± 0.16	0.29 ± 0.20
	II	Motor	a) primary	Precentral gyrus	4, 6	0.65	0.37 ± 0.20	0.29 ± 0.18
			b) pre-motor	Medial/superior frontal gyrus; cingulate gyrus	6; 24, 32	0.52	0.52 ± 0.18	0.46 ± 0.26
		Visual	a) medial	Cuneus, lingual gyrus, middle occipital gyrus	17, 18	0.72	0.30 ± 0.21	0.26 ± 0.16
			b) lateral	Fusiform gyrus, lingual gyrus, inferior occipital gyrus	17, 18	0.56	0.65 ± 0.16	0.35 ± 0.16
		Auditory		Superior temporal gyrus; insula	22, 41	0.79	0.20 ± 0.13	0.20 ±0.13
		Sensory-motor		Postcentral gyrus, inferior parietal lobule; medial frontal gyrus	1, 2, 3, 40; 6	0.64	0.31 ± 0.23	0.31 ± 0.19
	III	Parietal	a)	Inferior/superior parietal lobule	7, 40	0.55	0.38 ± 0.19	0.40 ± 0.24
			b)	Inferior parietal lobule	7	0.58	0.24 ± 0.15	0.22 ± 0.11
			c)	Angular gyrus; inferior parietal lobule	39; 40	0.62	0.17 ± 0.12	0.44 ± 0.21
		Precuneus	a)	Precuneus	7	0.54	0.49 ± 0.14	0.51 ± 0.20
			b)	Precuneus; cingulate gyrus, posterior cingulate; angular gyrus, middle temporal gyrus	31; 23, 30; 39	0.78	0.47 ± 0.17	0.54 ± 0.20
		Cingulate		Anterior cingulated	24, 32	0.64	0.14 ± 0.13	0.20 ± 0.16

AG: antonym generation task; VF: verbal fluency task; Similarity measure (*r*): spatial correlation coefficient between the CCOIs' maps across both tasks; Temporal correlation with reference (*r*): correlation coefficient between CCOIs' time courses and the reference function (mean ± STD across subjects), shown for CCOIs of each task separately in the last two columns. Activation regions and BAs of the language-specific CCOIs are listed separately for *ag1*, *ag2*, and *vf1*; those of the non-language-specific CCOIs are listed for both tasks together.

Table 2

the putative language ROIs for the ICA-derived language-specific CCOIs and the GLM results.

ICA-derived language-specific CCOIs					GLM results					
ca's Area		Wernicke's Area			Broca's Area			Wernicke's Area		
cent (%)	Total percent (%)	No. of voxels	ROI percent (%)	Total percent (%)	No. of voxels	ROI percent (%)	Total percent (%)	No. of voxels	ROI percent (%)	Total percent (%)
.5	6.4	0	0	0	176	67.7	3.6	5	0.7	0.1
5	1.2	108	15.9	7.6						
.2	9.8	5	0.7	0.3	91	35.0	5.3	0	0	0
.2	0.05	112	16.5	0.03	190	73.1	0.04	5	0.7	~0
.1	10.1	2	0.3	0.2	77	29.6	5.5	0	0	0

task. No. of voxels: the number of activated voxels within the language ROI; ROI percent (%): percentage of the activated voxels relative to the total
ent (%): percentage of the activated voxels within the ROI relative to the total number of activated voxels in the brain.